Influence of clay fraction on the shear behavior of an interface between sand-clay mixture and concrete

Kexin Yin, Anne-Laure Fauchille, Roxana Vasilescu, Christophe Dano, Panagiotis Kotronis, Giulio Sciarra

Influence of clay fraction on the shear behavior of an interface between sand-clay mixture and concrete

Kexin Yin[1, 2, *]

Anne-Laure Fauchille[2]

Roxana Vasilescu[3]

Christophe Dano[4]

Panagiotis Kotronis[2]

Giulio Sciarra[2]

Kexin Yin [1] Assistant Professor, Department of Civil Engineering, Nanjing University of Aeronautics and Astronautics, Nanjing 211106, China (corresponding author). E-mail: kexin.yin@nuaa.edu.cn

[2] Institut de Recherche en Génie Civil et Mécanique (GeM), Centrale Nantes, Nantes Université, 1 rue de la Noë 44321 Nantes Cedex 3, France

Anne-Laure Fauchille [2] Associate Professor, Institut de Recherche en Génie Civil et Mécanique (GeM), Centrale Nantes, Nantes Université, 1 rue de la Noë 44321 Nantes Cedex 3, France. E-mail: anne-laure.fauchille@ec-nantes.fr

Roxana Vasilescu [3] Research and Development Manager, PINTO SAS, 48 Rue Jules Verne, 35300, Fougères, France. E-mail: rvasilescu@pintogc.com

Christophe Dano [4] Associate Professor, 3SR, Université Grenoble Alpes, UMR CNRS 5521, Grenoble INP 38000, France. E-mail: christophe.dano@univ-grenoble-alpes.fr

Panagiotis Kotronis [2] Professor, Institut de Recherche en Génie Civil et Mécanique (GeM), Centrale Nantes, Nantes Université, 1 rue de la Noë 44321 Nantes Cedex 3, France. E-mail: panagiotis.kotronis@ec-nantes.fr

Giulio Sciarra [2] Professor, Institut de Recherche en Génie Civil et Mécanique (GeM), Centrale Nantes, Nantes Université, 1 rue de la Noë 44321 Nantes Cedex 3, France. E-mail: giulio.sciarra@ec-nantes.fr

Intended for publication in ***Journal of Geotechnical and Geoenvironmental Engineering***

ABSTRACT

In geotechnical engineering, the soil-structure interface is an important aspect to be taken into account in soil-structure interaction because it relates to the stability of supported structure. In particular, the shear behavior of the soil-structure interface plays a key role in the design of civil engineering structures and their analysis over time. The interface is a thin zone of soil in contact with the structure where major stresses and strains develop in. To our knowledge, previous works on the characterization of the mechanical behavior of the soil-structure interface mainly include typical soils (sand or clay) or natural soils, in contact with variable structural materials (concrete, steel, wood). However, natural soils are very complex, partly due to geological heterogeneities, and the mechanical response of typical soils do not always represent accurately intermediate soils between sand and clay. Previous studies on the mechanical behavior of those soils are significantly represented in the literature, especially in experimental research, however it is rather poorly documented on the interface between these soils and structural materials, whereas their response to mechanical loadings is different. The objective of this paper is to characterize the shear behavior of the soil-structure interface for intermediate soils between sand and clay, by experiments at the laboratory scale. Artificial mixtures of silica sand and kaolinite-rich clay are chosen to represent the intermediate soils in this study. For this propose, the research is organized in a main experimental campaign that aims to investigate the effect of the clay fraction, from 0% (sand) to 55% (kaolin clay) on the mechanical behavior of a soil-concrete interface by a new direct shear device in the laboratory. The characterization of the shear behavior of the soil-concrete interface at different clay and sand fractions allows to enlighten the role of soil microstructure at the soil-structure interface on the stability of civil engineering structures.

KEYWORDS:

Sand-clay mixture, clay fraction, soil-concrete interface, direct shear test, friction angle

1. Introduction

Soil-structure interface is of importance for the design and safety of geotechnical structures because it transfers the load from the structure to the surrounding soil. Soil-structure interface is a thin zone between the structure and the surrounding soil where major stresses and strains develop in (Maghsoodi 2020; Pra-Ai 2013; Pra-ai and Boulon 2017; Rouaiguia 2010), with a thickness usually a few times the mean particle size of the soils (Hu and Pu 2004; Pra-ai and Boulon 2017; Tovar-Valencia et al. 2018; Yin et al. 2021a). In the field, it is difficult to measure the intrinsic properties (i.e., adhesion c and interfacial friction angle δ) of the soil-structure interface, due to the long-time testing process, the heterogeneity of the stress state along the pile and the high installation costs. Moreover, there is still a lack of experimental understanding on how the interface behaves along loaded piles within sandy and clayey soils, due to the instrumentation restrictions along the piles at the engineering scale. Previous studies on the mechanical behavior of soil-structure interface mainly refer to model soils (e.g., sand or clay), without considering the fact that natural soils are generally composed of both sand and clay (Yin et al. 2021a). Since natural soils are complex and heterogeneous, it is difficult to gain well repeatable test results by using such soils for geotechnical tests. Reconstituted soils in terms of sand-clay mixtures are often employed in laboratory to investigate the mechanical behavior of natural soils. Literature on the mechanical interface behavior of sand-clay mixtures and structure is poorly documented (Yin et al. 2021a). Direct interface shear tests are usually used to study the mechanical behavior of soil-structure interface (Li et al. 2019; Maghsoodi et al. 2020a; Martinez and Stutz 2019; Vasilescu 2019; Yazdani et al. 2019; Yin et al. 2021c; Yin et al. 2020), since it can be easily and economically performed in laboratory. There are plenty of direct shear tests performed on reconstituted sand-clay mixture soils in the literature (Balaban et al. 2019; Dafalla 2013; Kim et al. 2018; Monkul and Ozden 2007; Shahin et al. 2020), however very few results focus on the direct

shear results of the interface between sand-clay mixtures and structural materials. For example, Aksoy et al. (2016) carried out direct shear tests to obtain the internal and interface friction angles of the sand-clay mixtures. The results show that the interface friction angles of both soil-steel and soil-wood are lower than the internal friction angles of sand-clay mixtures, but the details about the interface roughness is not given. An experimental investigation of interface direct shear tests was performed by Li et al. (2020) to study the shear behavior at the interface between a sand-bentonite mixture and a smooth geomembrane under the condition of freeze-thaw cycles. The test results indicate that the shear strength at the interface is lower than that of the mixture itself, and the shear strength decreases with increasing numbers of freeze-thaw cycles. However, these results fail to provide a comprehensive understanding on the mechanical response of the sand-clay mixtures even though they point out that the clay content affects the shear behavior of the mixtures. The influence of clay content on interface behavior and particles arrangement in not clear (Yin et al. 2021a). Implementing direct shear tests on sand-clay mixture-structure interface is necessary to better understand the mechanical characteristics of natural soil-structure interfaces.

In this paper, the mechanical behavior of soil-structure interface is investigated by a new interface direct shear device. To represent the interface of a pile foundation in natural soil, reconstituted sand-clay mixtures at controlled clay fractions and a concrete plate are chosen for the soil and structural material. The effect of the clay fraction, from 0% (sand) to 55% (kaolin clay), on the mechanical response of the sand-clay mixture-concrete interface is therefore investigated.

2. Experimental apparatus

2.1 Interface direct shear machine

The mechanical behavior of the sand-clay mixture-concrete interface is investigated experimentally using a new interface direct shear apparatus at Ecole Centrale Nantes (France), adapted to a large range of soils, and validated by Vasilescu (2019). This machine is designed to characterize shear behavior of soil-structure interfaces in laboratory (Fig. 1). Its shear box can contain geological soil and structural material. A concrete plate (Fig. 1d) is used to simulate the pile material in Fig. 1a, embedded in the lower part of the shear box. The soil specimen in the shear box (Fig. 1b) can be a dry or saturated soil remolded or taken from the field. This machine (Fig. 2) offers the capability of conducting shear tests by imposing monotonic/cyclic mechanical and thermal loadings (note that, in this study, this part of the system is only used to apply and maintain a constant temperature). The device is designed for conducting tests with three boundary conditions: constant normal load (CNL), constant volume (CV), and constant normal stiffness (CNS).

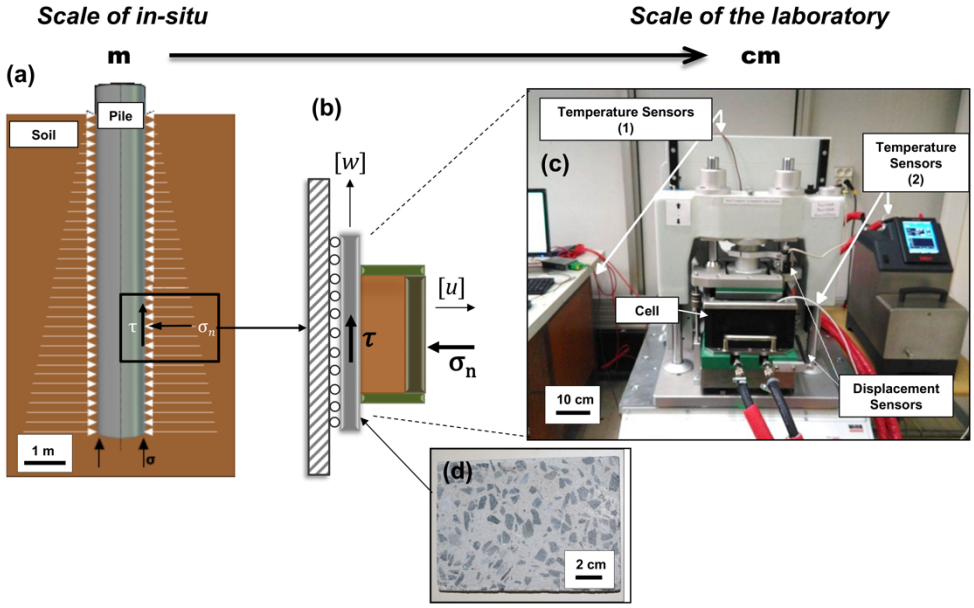

Fig. 1 Soil-structure interface: (a) schematic at in-situ scale, (b) schematic of the interface direct shear box at laboratory scale, (c) the interface direct shear machine in laboratory, and (d) a concrete plate.

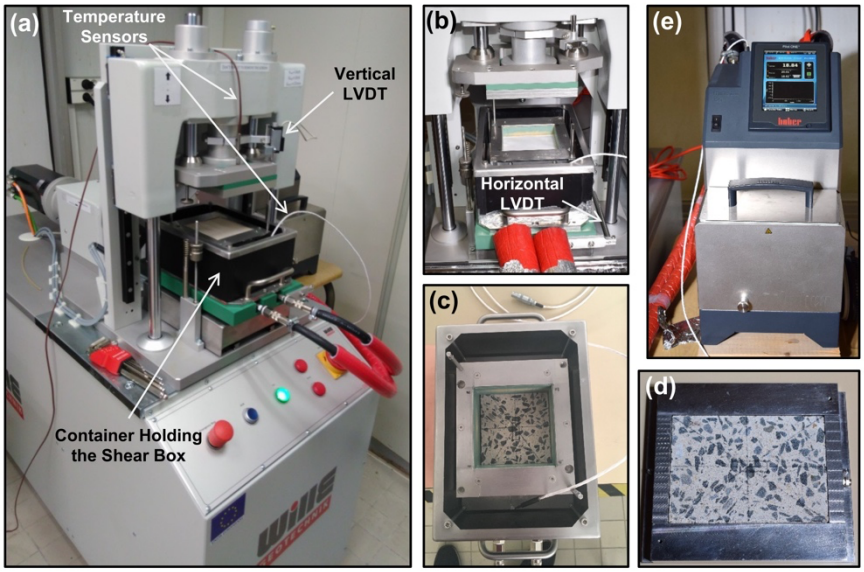

Fig. 2 Interface direct shear test apparatus: (a) loading frame and electromechanical force actuators, (b) zoom of the main loading part, (c) container with the shear box and concrete plate, (d) lower part of the shear box and concrete plate and (e) refrigerated heating circulator bath with air-cooled cooling machine.

In general, a classical direct shear box is equipped with an upper part and a lower part of the same size. Classical shear box for direct shear tests on soil-soil results however in a varying contact area between the two parts of soil sample during shearing. An ad-hoc new design is therefore proposed so that a constant shearing area is maintained over the specified range of displacement, to prevent rotation of the upper box and spurious friction component during shearing on soil-structure interface. The square interface shear box is divided in two parts, subsequently referred to as the upper part and the bottom part (Fig. 2c, d), which are independent in terms of movement. The dimension of the upper part is 100 mm × 100 mm and can accommodate soil samples with a maximum initial height of 50 mm. The bottom part can contain soil specimens or structural elements with a dimension of 140 mm × 100 mm × 11 mm and has a temperature sensor in its lower part. The whole shear box is installed in a container (see Fig. 2a, c) that can be filled with distilled water for testing saturated specimens and possibly guarantee a homogeneous thermal equilibrium. During shearing, the

upper part of the shear box is fixed by the piston that applies the vertical load and cannot move, while the lower part moves horizontally, imposing a relative displacement.

The vertical (i.e., normal) and horizontal (i.e., shear) loads are imposed by two electromechanical force actuators. A load cell is installed on each actuator to accurately measure both vertical and horizontal loads applied on the specimen (Fig. 2a, b). Two Linear Voltage Displacement Transducers (LVDTs) are used to measure horizontal and vertical displacements (Fig. 2a, b). As shown in Table 1, the vertical load cell provides normal force with a capacity of 10 kN while the horizontal load cell can impose a maximum shear force of ±10 kN; the two load cells have an accuracy of 0.1% of the measuring range. The maximum vertical and horizontal displacements are ±5 mm and ±20 mm respectively (with an accuracy of 0.1% of the measuring range). The apparatus allows to choose a load-controlled shear mode or a displacement-controlled shear mode. The frequency for the cyclic test option ranges between 0 and 10 Hz. The maximum amplitude of horizontal displacement at the frequency of 1 Hz is ±5 mm, and at the frequency of 5 Hz is ±1 mm.

Table 1 Characteristics of the sensors.

Sensor	Operating range	Accuracy
Vertical load cell	0 ~ 10 kN	0.1%
Horizontal load cell	0 ~ ±10 kN	0.1%
Vertical LVDT	±5 mm	0.1%
Horizontal LVDT	±20 mm	0.1%
Pt100 temperature sensor	0 ~ +50°C	0.2°C

3. Materials

3.1 Fontainebleau sand

Fontainebleau sand NE34 (Fig. 3a) from Sibelco® company (France) was selected to prepare reconstituted sand-clay mixture. It is composed of 99% quartz according to energy dispersive spectrometer (EDS) analyses. Grain size distribution curve is presented in Fig. 4a, which corresponds to typical results in literature, with grain sizes below 500 μm. Grains have a sub-

rounded shape. The specific gravity is 2.65. It is characterized with a mean grain size (d_{50}) of 0.21 mm, a coefficient of uniformity (C_u) of 1.72. Its maximum and minimum void ratio is equal to 0.866 and 0.545, respectively (Maghsoodi et al. 2020b; Pra-Ai 2013; Vasilescu et al. 2019).

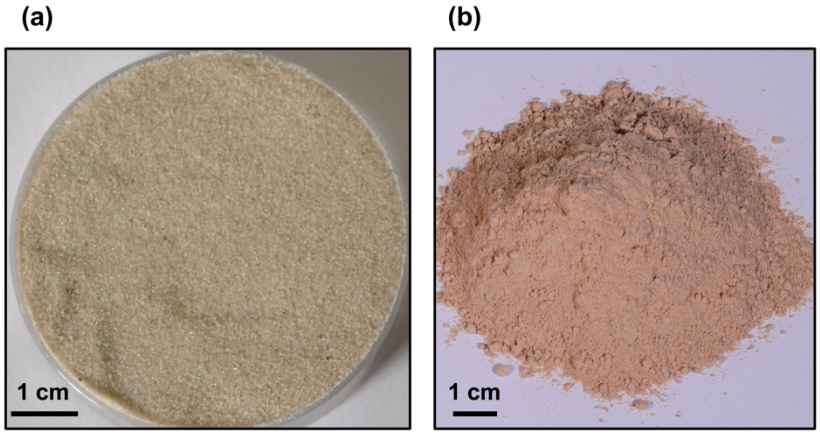

Fig. 3 (a) Fontainebleau sand NE34 and (b) kaolin clay.

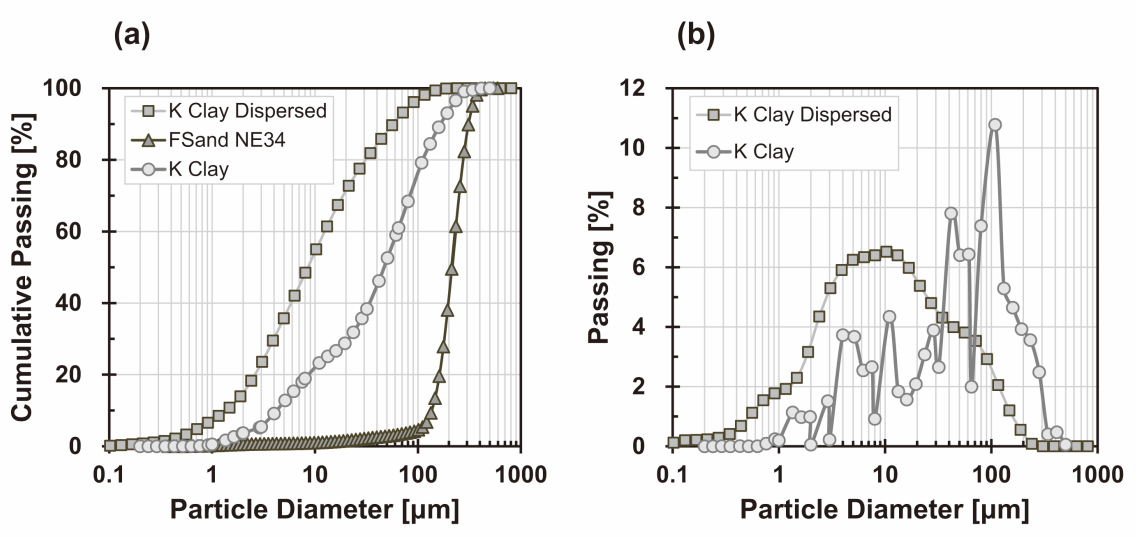

Fig. 4 (a) Grain size distribution of Fontainebleau sand and kaolin clay represented by the cumulative passing as a function of particle diameter and (b) passing fraction as a function of particle diameter for the dispersed and non-dispersed kaolin clay.

3.2 Kaolin clay

A kaolin clay (Fig. 3b) from Argeco® company (France) was adopted as clay material. The kaolin is composed of 55% kaolinite minerals (Aboulayt et al. 2018; San Nicolas et al. 2013)

and well-dispersed quartz particles (Yin et al. 2021b; Yin et al. 2019). Atterberg limit tests on the kaolin clay was performed by using a Casagrande apparatus and the thread twisting method in the laboratory. The liquid (w_L) and plastic (w_P) limits of the clay are 37.3% and 19.0%, respectively (plasticity index PI = 18.3%). Curves of grain size distribution are given in Fig. 4. The grain size distribution tests were conducted by using two laser granulometers on dispersed and non-dispersed kaolin clay. The dispersed kaolin clay was dispersed by distilled water in sample dispersion units before measuring, whereas the non-dispersed one was dry kaolin clay powder. The comparison of passing fractions before and after dispersion reveals that clayey aggregates are present in the kaolin clay, and they are then scattered by the dispersion process. The mean grain size d_{50} of the dispersed and non-dispersed kaolin clay is 8.6 μm and 47.5 μm, respectively.

3.3 Concrete plate

3.3.1 Mixing design

Concrete was selected as the structural material. As summarized in Table 2, the concrete was prepared by mixing the cement, limestone filler, sand (0 ~ 4 mm), aggregates (6 ~ 10 mm), and distilled water according to Eurocode-2 (2004). After mixing, the concrete was moved to a mould and under steam curing for 28 days. Several slices of concrete plates with a size of 140 mm × 100 mm × 11 mm were cut from the concrete block for interface tests (Fig. 5).

Table 2 Mix design of the concrete.

	Cement (kg/m^3)	Sand (kg/m^3)	Aggregate (kg/m^3)	Limestone filler (kg/m^3)	Water (kg/m^3)
Values	330.0	707.4	950.6	210.0	212.1

Fig. 5 The concrete plate.

3.3.2 Surface roughness

Roughness parameters were measured by a Taylor Hobson Surtronic 3+ surface roughness tester before and after shearing tests. The roughness test was performed on two directions of the plate surface: six testing profiles in the shear direction and eight profiles perpendicular to the shear direction. The tester measured the roughness parameters of all profiles, and the mean values were calculated. Normalized roughness (R_n) is used for evaluating the interface roughness, it is defined as

$$R_n = \frac{R_{max}}{d_{50}} \quad (1)$$

where R_{max} is the peak-to-valley height that can be obtained by measuring the maximum vertical distance between the highest and lowest peak of the structure asperities along an evaluation profile length L_n (Gadelmawla et al. 2002; ISO 1997; Uesugi and Kishida 1986a; Uesugi and Kishida 1986b; Yin et al. 2021a).

The average R_{max} and R_a (arithmetic average of the absolute values of the profile heights over the evaluation length along the center line) of the concrete plate are 92.0 μm and 10.3 μm, respectively (Table 3). The R_n between the concrete plate and Fontainebleau sand, kaolin clay, and dispersed kaolin clay, is listed in Table 3. For sand, the concrete surface is medium rough (Hu and Pu 2004; Lings and Dietz 2005; Maghsoodi 2020; Maghsoodi et al. 2019;

Uesugi et al. 1989), while for dispersed and non-dispersed kaolin clay, it is a high rough surface (Maghsoodi 2020; Maghsoodi et al. 2019). Concerning the sand-clay mixtures, the surface can be regarded as rough.

Table 3 Roughness parameters.

	R_a (μm)	R_{max} (μm)	d_{50} (μm)	R_n (μm)	Surface roughness
Fontainebleau sand	10.3	92.0	210	0.426	Medium rough
Kaolin clay	10.3	92.0	47.53	1.883	High rough
Kaolin clay dispersed	10.3	92.0	8.56	10.458	High rough

Only one concrete plate was used for all shear tests. The R_{max} and R_a were 90.5 μm and 10.2 μm after all the interface shear tests. The results thus confirmed the assumption that the shear tests did not significantly alter concrete roughness, which is in agreement with previous publications (Tsubakihara et al. 1993; Vasilescu 2019).

4. Experimental setup

In this section, the sample preparation as well as the experimental plan of the interface direct shear test on sand-clay mixture and concrete is presented. The sample preparation protocol, initial sample properties and loading conditions are detailed.

4.1 Sample preparation

4.1.1 Atterberg limits

Atterberg limit tests of sand-clay mixtures with a series of kaolin clay content (i.e., 25%, 50%, 60%, 75%, 100%) were performed by using a Casagrande apparatus and the thread twisting method to get the liquid limit (w_L) and plastic limit (w_P), respectively. Plasticity index (PI) of the sand-clay mixtures were calculated with the values of liquid and plastic limits. As mentioned before, this kaolin clay has a 55% by weight of real clay from the size distribution point of view (<2 μm), so we multiply 55% on the kaolin clay content to get the

239 actual clay fraction (the similar ones that will follow). In the following, the clay fraction is
240 expressed based on the clay definition of particles less than 2 μm.
241 The results in Table 4 show the Atterberg limits of the sand-clay mixtures have a linear
242 relationship with the kaolin clay content or clay fraction, corresponding to the literature
243 (Hattab et al. 2015; Polidori 2007; Seed et al. 1966). The initial water quantity used for
244 sample preparation is set up with a criterion ($1.5w_L$, see the following section) based on the
245 liquid limits of the sand-clay mixtures at each clay fraction. It is noted that at the clay fraction
246 of 13.75%, there are not any values for the plastic limit and plasticity index (Table 4), since
247 the clay quantity in the mixture is quite small, the measurement of the plastic limit is
248 impossible.

249 **Table 4 Atterberg limits of the sand-clay mixtures.**

Kaolin clay content (%)	Clay fraction (%)	w_L (%)	w_P (%)	Plasticity index (-)
25	13.75	17.9	-	-
50	27.5	22.4	13.7	8.7
60	33	26.8	14.4	12.4
75	41.25	31.0	15.2	15.8
100	55	37.3	19.0	18.3

250

251 *4.1.2 Sample preparation*

252 The sample preparation is a key factor that influences the mechanical behavior of
253 reconstituted soils (Carraro and Prezzi 2008; Krage et al. 2020; Wang et al. 2011; Wichtmann
254 et al. 2020), especially for clayey soil samples. It is necessary to utilize an adapted procedure
255 for the sample preparation to guarantee an optimized sample homogeneity of sand-clay
256 mixtures. A specific sand clay mixing protocol is proposed to prepare the sand-clay mixture
257 slurry (see Yin et al. (2019), Yin et al. (2021b) and Yin et al. (2021d)). It consists in mixing
258 successively dry Fontainebleau sand, distilled water and kaolin clay powder at an initial water
259 content of 1.5 times the liquid limit of the sand-clay mixture (Table 4). The procedure is
260 proved to be suitable for the interface direct shear apparatus, which is capable to guarantee a
261 good homogeneity of the sand-clay mixture samples, in terms of the distribution of phase

components, water content, density and mechanical parameters (see Yin et al. (2021b) and Yin et al. (2021d)).

After the sand, distilled water and kaolin clay are mixed into a slurry, it is transferred to an oedometer cell and subjected to a preconsolidation phase in saturated conditions. The constant normal loading steps are 5.59 kPa, 25 kPa, 37.5 kPa, and 50 kPa (Yin et al. 2021d). Then the preconsolidated specimen is trimmed down to an adequate dimension for the interface shear box. The water content, the mass and the initial height of the sample are measured. More details about the sample preparation and designed oedometer cell can be referred to Yin et al. (2021b) and Yin et al. (2021d).

4.2 Experimental plan

4.2.1 Direct shear test

Direct shear test on sand and clay are performed on the interface direct shear device as references, to compare with the interface results. The sand and clay samples are prepared by dry tamping method in the shear box layer by layer, without the concrete plate in the shear box. The samples are firstly consolidated and after that a displacement-controlled shear is carried out. The normal stresses are 20 kPa (only for sand), 50 kPa, 100 kPa and 150 kPa and loaded with a rate of 50 kPa/min. After reaching the target vertical stress, distilled water is instantly added into the container to submerge the sample and guarantee a saturated condition. Then a constant temperature of 18.6℃ is set, which corresponds to the average room temperature of the laboratory over a year. The shear velocity for the sand and clay are 0.1 mm/min and 0.005 mm/min respectively, to ensure a drained shear. The total horizontal (shear) displacement is 10 mm for sand, and 8 mm ~ 12 mm for clay, which is enough to get a constant ultimate volumetric state. The sample parameters of the conventional direct shear tests are presented in Table 5.

Table 5 Sample properties of Fontainebleau sand and kaolin clay for the conventional direct shear tests on soil-soil.

Test name	Normal effective stress (kPa)	Sample mass (g)	Height (mm)	Sample density (g/cm^3)	Void ratio (-)
Sand_20kPa	20	601.26	32.80	1.61	0.642
Sand_50kPa	50	601.01	32.85	1.61	0.645
Sand_100kPa	100	602.34	33.80	1.57	0.683
Sand_150kPa	150	603.44	31.53	1.68	0.580
Clay_50kPa	50	587.77	48.10	1.12	1.369
Clay_100kPa	100	607.70	50.55	1.10	1.399
Clay_150kPa	150	609.21	51.59	1.09	1.438

4.2.2 Interface direct shear test

The kaolin clay contents of the interface direct shear experiments are 0%, 25%, 40%, 50%, 60%, 75%, 100% by weight. In other words, the clay fraction (i.e., real clay content) is 0%, 13.75%, 22%, 27.5%, 33%, 41.25% and 55%. The normal stresses are 50 kPa, 100 kPa and 150 kPa that correspond to typical normal effective stresses acting on soil-pile interfaces at specific depths for bored or driven pile foundations. The sand-clay mixture samples are prepared by the method presented above and normally consolidated (NC). The initial properties of the samples are collected in Table 6. The samples of 100% sand content are prepared by dry tamping.

Table 6 Sample properties after preconsolidation for the soil-concrete interface direct shear tests.

Test name	Sample mass (g)	Height (mm)	Water content (%)	Density (g/cm^3)	Void ratio (-)	S_r (%)
0%Clay_50kPa	401.40	24.21	-	1.66	0.598	-
0%Clay_100kPa	401.09	24.02	-	1.67	0.586	-
0%Clay_150kPa	400.91	24.13	-	1.66	0.595	-
13.75%Clay_50kPa	508.79	23.18	20.21	2.19	0.451	100
13.75%Clay_100kPa	497.78	23.48	20.30	2.12	0.504	100
13.75%Clay_150kPa	506.71	24.15	20.49	2.10	0.522	100
22%Clay_50kPa	631.86	30.62	19.67	2.06	0.537	97.09
22%Clay_100kPa	632.05	30.11	19.11	2.10	0.504	100
22%Clay_150kPa	618.52	29.80	19.74	2.08	0.528	99.02
27.5%Clay_50kPa	622.72	30.59	20.01	2.04	0.562	94.37
27.5%Clay_100kPa	644.66	31.23	20.10	2.06	0.542	98.35
27.5%Clay_150kPa	647.72	31.56	20.59	2.05	0.557	97.98
33%Clay_50kPa	524.02	25.90	22.56	2.02	0.605	98.83

33%Clay_100kPa	511.29	25.58	22.35	2.00	0.622	95.27
33%Clay_150kPa	509.98	25.35	21.91	2.01	0.606	95.83
41.25%Clay_50kPa_a	530.32	26.80	27.29	1.98	0.704	100
41.25%Clay_50kPa_b	531.87	26.94	25.83	1.97	0.689	99.42
41.25%Clay_100kPa_a	544.63	27.71	25.53	1.97	0.692	97.78
41.25%Clay_100kPa_b	523.94	26.85	25.19	1.95	0.700	95.42
41.25%Clay_150kPa_a	530.48	27.01	24.95	1.96	0.686	96.42
41.25%Clay_150kPa_b	531.55	27.18	25.41	1.96	0.699	96.30
41.25%Clay_150kPa_c	530.15	27.03	25.07	1.96	0.690	96.31
55%Clay_50kPa_a	523.18	28.15	30.32	1.86	0.858	93.61
55%Clay_50kPa_b	555.90	30.87	32.78	1.80	0.953	91.10
55%Clay_100kPa	545.08	29.10	30.49	1.87	0.846	95.51
55%Clay_150kPa	540.61	29.06	32.33	1.86	0.885	96.81

It is impossible to check the saturation degree (S_r) at the end of the consolidation stage on the interface shear machine. Thus, just the degree of saturation S_r after the preconsolidation in the sample preparation procedure is checked. In Table 6, most of the S_r values of the specimens are greater than 95% and thus they are considered as saturated (Di Donna 2014). More, the samples are submerged in distilled water in the container during the whole test steps, to ensure the direct shear test is performed under saturated conditions.

4.3 Loading conditions

4.3.1 Vertical loading

After adding the first step of the normal stress on the sample, distilled water is added into the shear box container, then the temperature of the sample is set as a constant at 18.6℃, to obviate the thermal influence on test results. The normal load is added by a step loading procedure, as illustrated in Fig. 6. At each step, the vertical loading rate is 50 kPa/min. Each consolidation step is maintained until the normal deformation is stable then the next vertical stress is applied, see Fig. 6. After the vertical displacement of the specimen is stable, the Constant Normal Load (CNL) boundary condition is employed for the interface direct shear tests. When the changing rate of vertical displacement is less than 0.005 mm/h or the vertical strain rate is less than 0.2% per hour, the vertical deformation is considered stable, the

consolidation process is stopped, and the following loading step starts (ASTM-D2435 2011; Li et al. 2019).

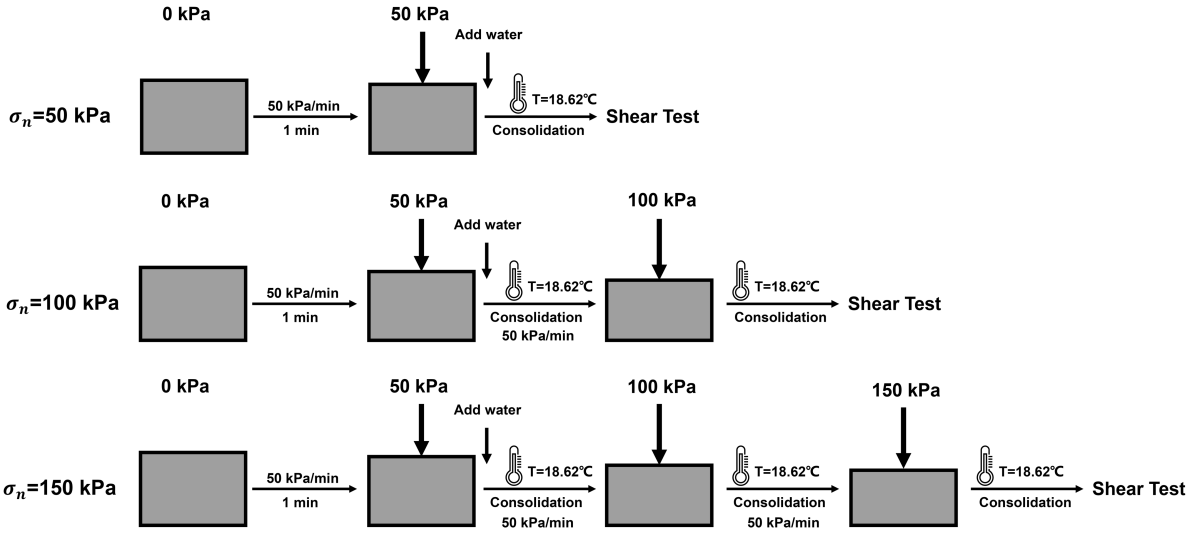

Fig. 6 Schematic diagram of the step vertical loading procedure.

4.3.2 Shearing velocity

Displacement-controlled interface shear tests are performed using a horizontal displacement-controlled mode at a rate of 0.005 mm/min. The specimen is sheared to a total horizontal displacement of 5 mm, which is enough to reach a constant volume state, then sheared from 5 mm back to 0 mm (initial position). This shearing rate is small enough and can ensure a totally drained shearing, it is chosen in accordance with ASTM-D3080 (2011) to ensure that excess pore water pressure is dissipated during shearing.

5. Results

5.1 Direct shear test

5.1.1 Fontainebleau sand

The results of direct shear tests performed on Fontainebleau sand are presented in Fig. 7. The mobilized shear stress-horizontal displacement curves indicate that for a specific initial sample density of dense state, the sand undergoes a peak phase before reaching a constant volume (residual) state at relatively high normal stress (100 kPa and 150 kPa) while the peak

is less apparent at low normal stress of 20 kPa and 50 kPa (Fig. 7a, b). This result is consistent with the literature (Vasilescu 2019) and can be read thinking of the behavior of dense sands which exhibit a contractive then a dilative volumetric response to direct shear loading, accompanied by a peak and a residual stress. According to the curves on vertical strain in Fig. 7c, the sand slightly contracts for horizontal displacements lower than 1.0 mm and then dilates. This volumetric behavior is consistent with typical direct shear response of dense sand (Di Donna et al. 2016; Hu and Pu 2004; Vasilescu 2019).

The peak internal friction angle (φ_{peak}) is 40.4°, and the internal friction angle at the constant volume condition (residual) φ_{cv} is 33.7° (Fig. 7b), which is 2.2° lower than the values of 35.9° from the same machine and 2.5° lower than the 36.2° from a conventional direct shear device in Vasilescu (2019), but in dry condition and a shear rate of 1.27 mm/min. This difference is induced by the size effect of the shear box (Cerato and Lutenegger 2006; Wang and Gutierrez 2010; Wu et al. 2008), related to the progressive failure from the ends to the central part of the interface, therefore related to the dimensions of the shear box: the shear box of the classical device has a smaller size (60 mm × 60 mm), compared to the one on the interface machine (100 mm × 100 mm). Larger shear box provides more space for sand grains to rearrange and fully develop a constant volume state (Cerato and Lutenegger 2006; Dadkhah et al. 2010). To sum up, the results of direct shear test on sand-sand under saturated condition is consistent with previous results with/without water (Maghsoodi 2020; Maghsoodi et al. 2020b; Pra-ai and Boulon 2017; Vasilescu 2019; Yavari et al. 2016).

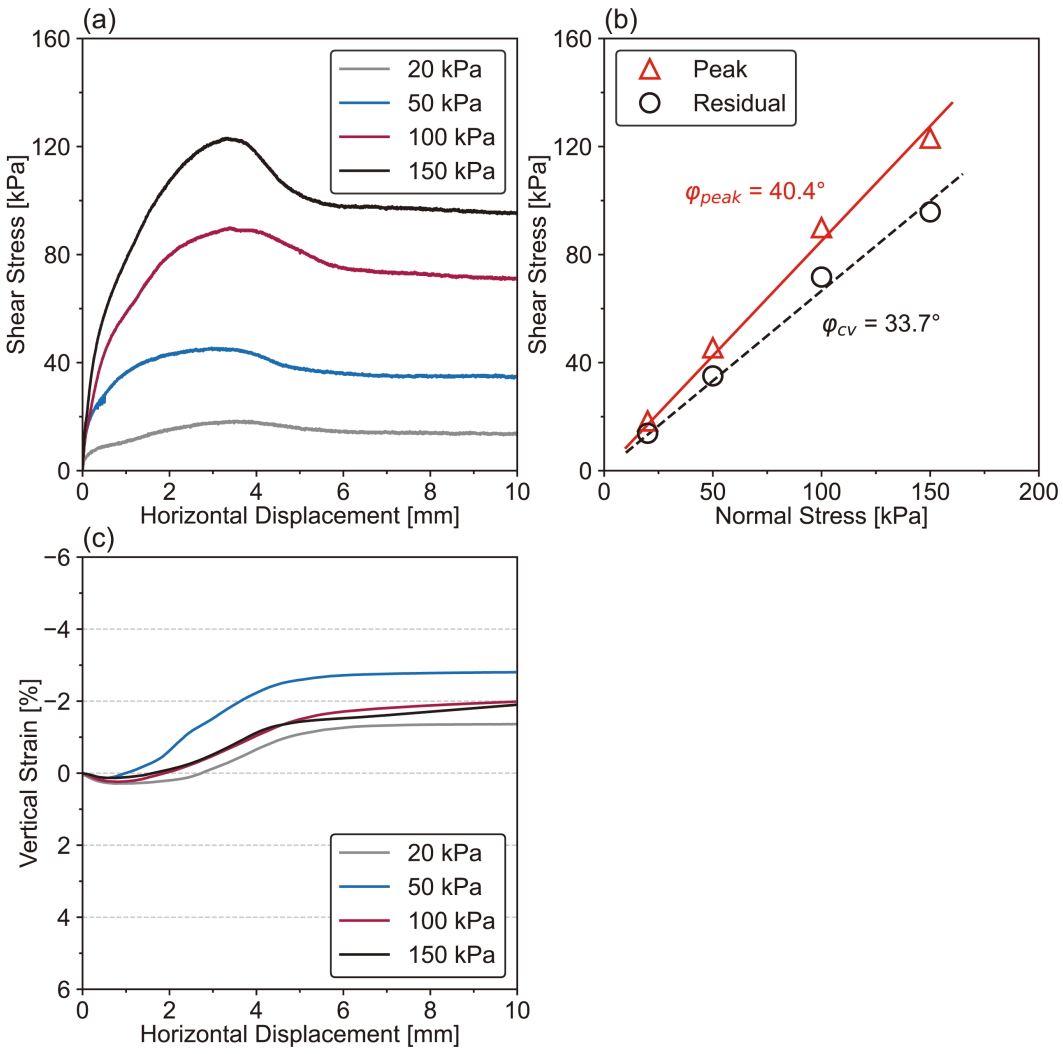

Fig. 7 Direct shear test results of saturated Fontainebleau sand-Fontainebleau sand: (a) shear stress as a function of horizontal displacement, (b) Mohr-Coulomb envelopes, and (c) volumetric strain (positive values mean contraction and the similar ones that will follow) as a function of horizontal displacement.

5.1.2 Kaolin clay

For direct shear tests on saturated pure kaolin clay, shear stress-horizontal displacement, Mohr-Coulomb envelopes and volumetric deformation are represented in Fig. 8. The specimens are normally consolidated clay thus the shear stress curves do not show any distinct peaks. The bottom part of the shear box contains a few canals (seen as small holes) to allow water injection into the sample to allow a well distributed saturation. In the case of interface experiments, the end of those canals is covered by the concrete plate, whereas in direct shear experiments, there is not a concrete plate in the groove to cover. When shearing

the clay, a part of the clay particles might go to these holes, and due to this reason, shear stress drops can be observed on the curves in in Fig. 8a. This phenomenon is interpreted as a boundary effect induced by the shear box characteristics, and it tends to disappear when approaching residual state. The clay contracts without dilatancy during the entire shear tests (Fig. 8c), the maximum vertical strain increases with the normal stress (Fig. 8c). The contraction increases until the end of the test which is similar to the clay CNL direct shear test in Maghsoodi et al. (2020b).

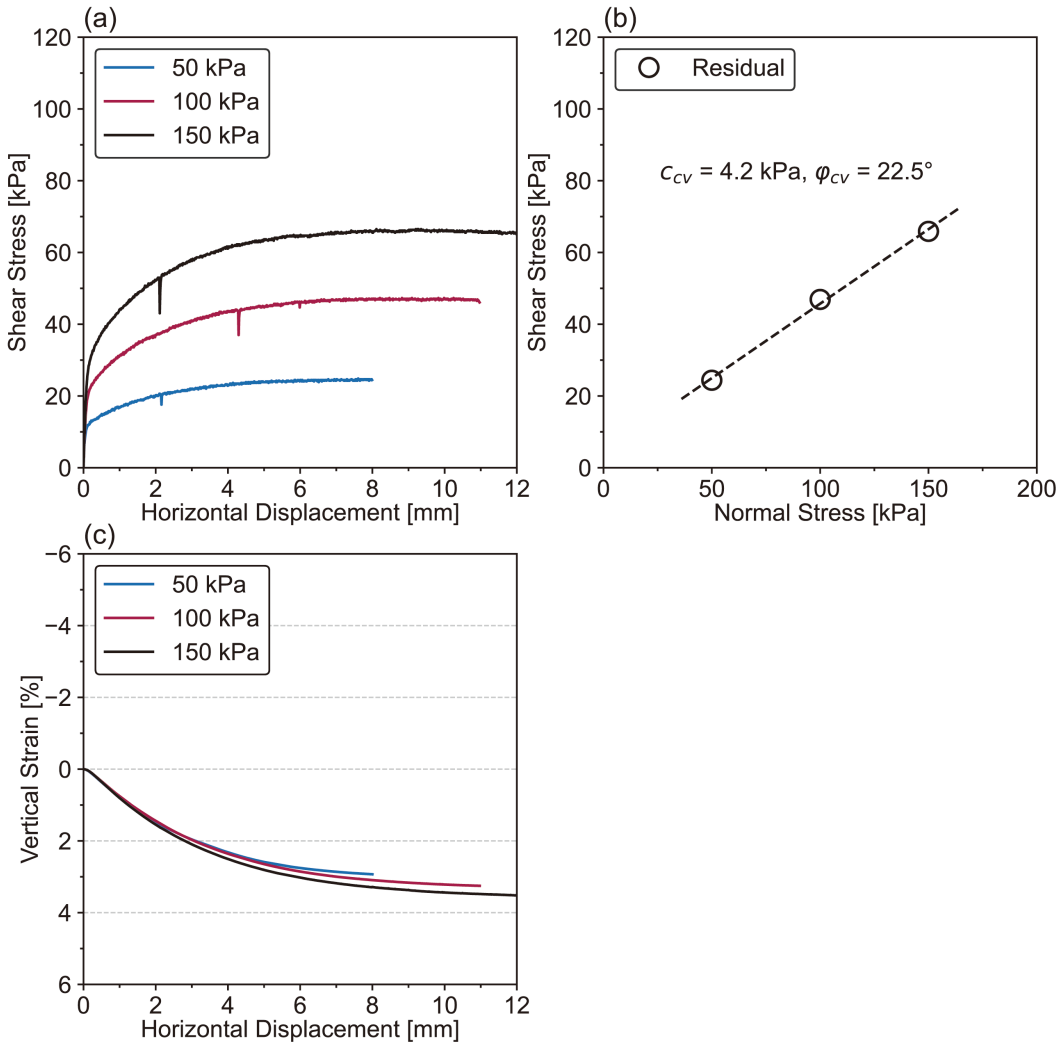

Fig. 8 Direct shear test results of saturated kaolin clay-kaolin clay: (a) shear stress as a function of horizontal displacement, (b) Mohr-Coulomb envelope, and (c) volumetric strain as a function of horizontal displacement.

The cohesion of this kaolin clay at constant volume condition (4.2 kPa, see Fig. 8b) is in good agreement with previous direct shear results on kaolin clay in Yavari et al. (2016). The value of cohesion is quite small (<5 kPa) since the tested specimens are highly saturated NC clay. The residual internal friction angle is 22.5° (Fig. 8b), in accordance with previous publications (Rouaiguia 2010; Yavari et al. 2016).

5.2 Interface direct shear test

This section presents the interface shearing results to clarify the influence of clay fraction on the shear behavior of the sand-clay mixture-concrete interface.

5.2.1 Shear stress and volumetric deformation

Shear stress as a function of horizontal displacement is exhibited in Fig. 9. As expected, the shear strength increases with normal stress, while it might either increase or decrease with clay fraction. At the clay fraction of 0%, there are small peaks on the shear stress curves at normal stresses of 50 kPa, 100 kPa and 150 kPa. For the tests of other clay fractions, no obvious peaks are found because the specimens are fully saturated and normally consolidated.

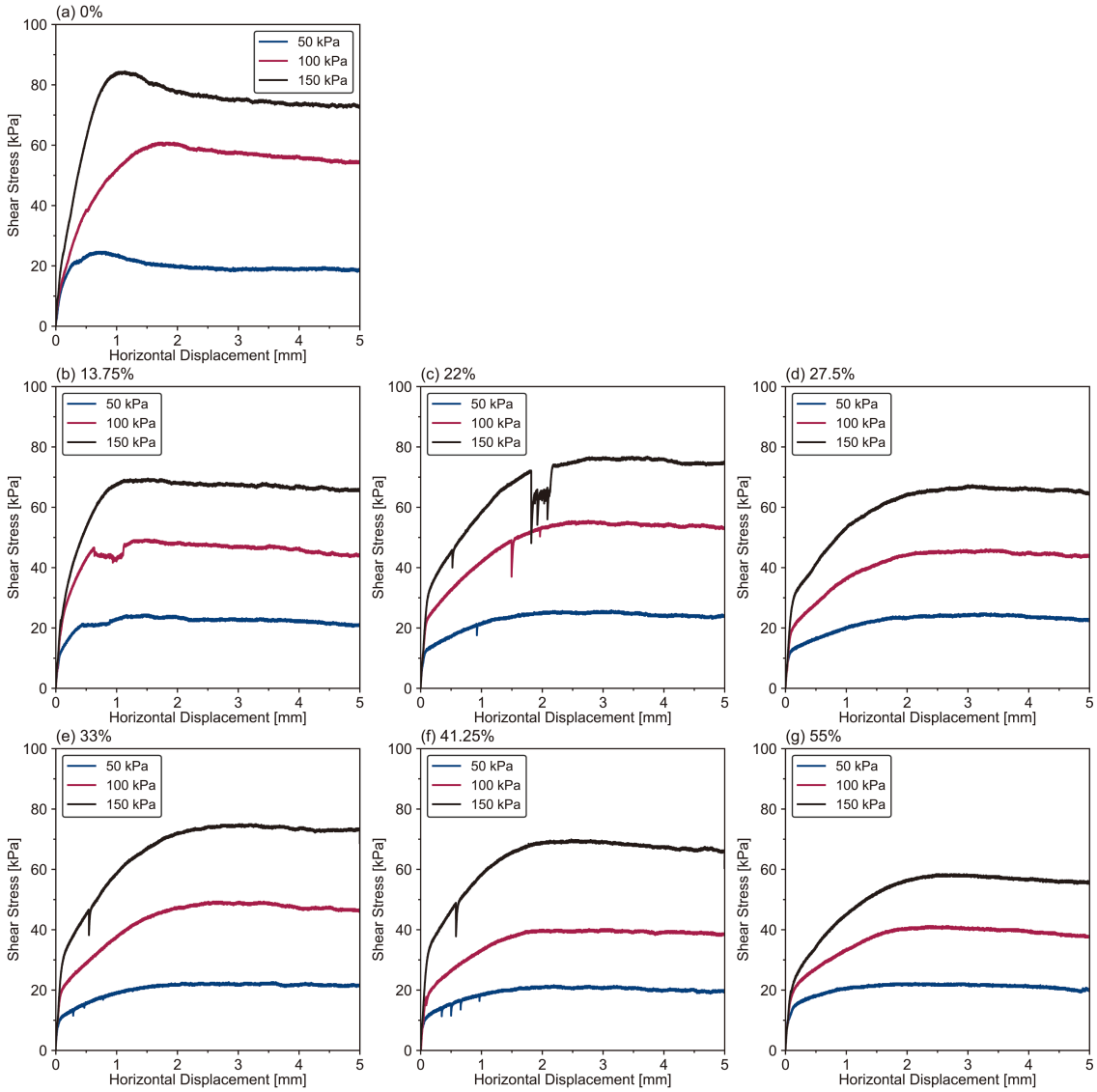

Fig. 9 Shear stress as a function of horizontal displacement at (a) 0%, (b) 13.75%, (c) 22%, (d) 27.5%, (e) 33%, (f) 41.25% and (g) 55% clay fractions.

The results in Fig. 9c (22% clay fraction, 150 kPa normal stress) illustrate a sudden collapse of the shear stress that can probably be explained with an unstable matrix structure in sand-clay mixture at this clay fraction because it is near the transitional clay content FC_t (Monkul and Ozden 2005; Monkul and Ozden 2007; Yin et al. 2021a; Zuo and Baudet 2015). Part of the intergranular contact between sand grains are bridged by clay particles and then a metastable state is formed. Some of the intergranular bridges dislodge and thus a sudden collapse takes place during shearing. Another reason for this shear stress drop is that a part of the soil particles goes into the small pits on the concrete plate surface during the shearing.

However, this sudden collapse does not affect the total trend of the shear stress curve and the residual shear strength (Fig. 9b, c).

The volumetric deformation in terms of vertical strain is presented in Fig. 10. The curves of the three normal stresses in 0% and two normal stresses (50 kPa, 100 kPa) in 13.75% clay fraction groups show a first contraction then dilation response during shearing. The response of volumetric deformation under the three normal stresses is very close, at the clay fractions of 22%, 27.5%, 33% and 41.25%.

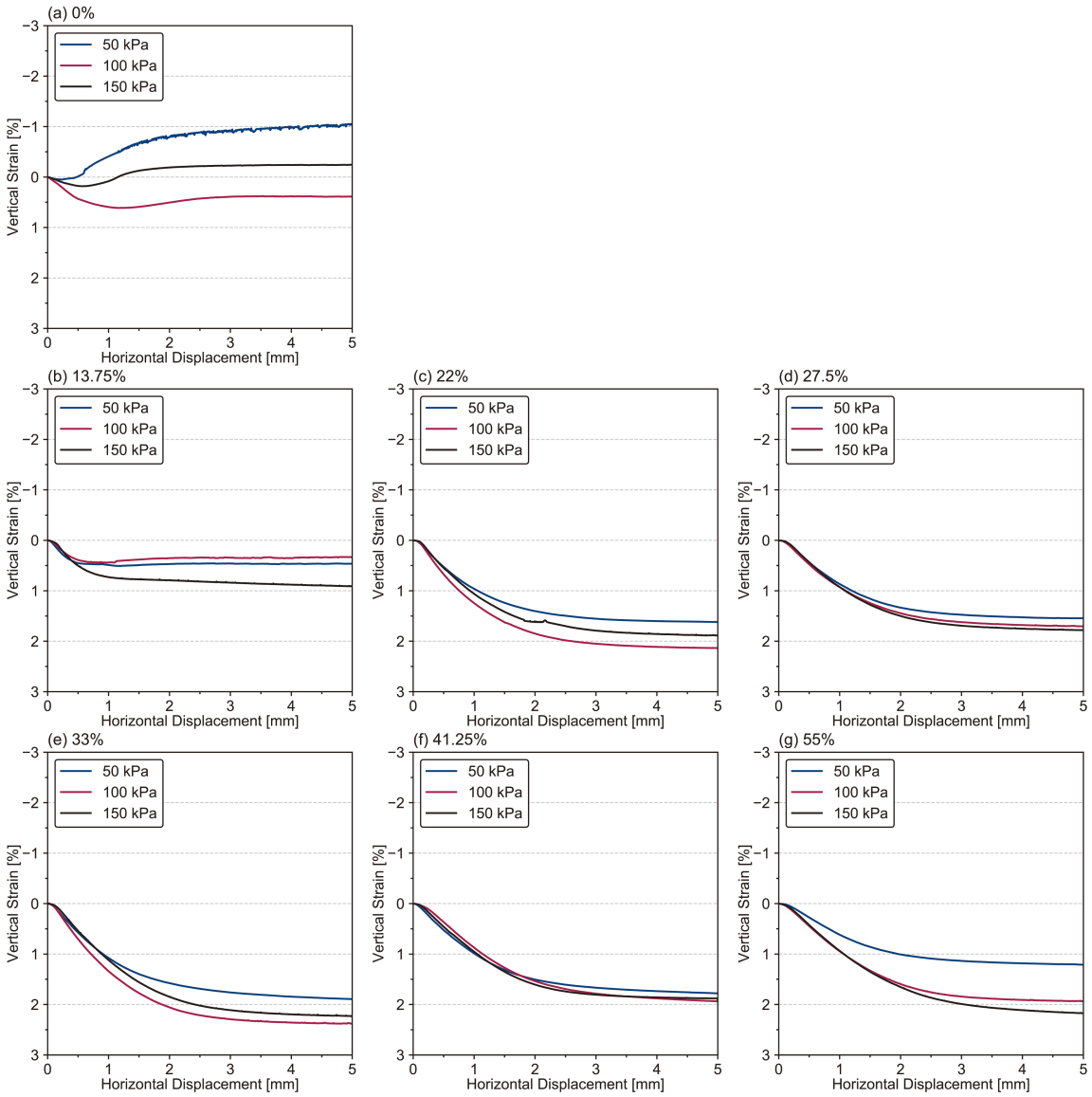

Fig. 10 Vertical strain as a function of horizontal displacement at (a) 0%, (b) 13.75%, (c) 22%, (d) 27.5%, (e) 33%, (f) 41.25% and (g) 55% clay fractions.

The vertical deformation is also expressed by the void ratio variation. From the beginning of consolidation to the end of shear, the void ratio versus the normal stress is presented in Fig. 11. The void ratio decreases with increasing normal stress in the consolidation process, and it reveals that the tests are repeatable. During the CNL shearing in Fig. 11, the void ratio continues to decrease (50 kPa: from 0.472 to 0.449; 100 kPa: from 0.433 to 0.409; 150 kPa: from 0.403 to 0.378), indicating a contraction tendency in agreement with Fig. 10d. The Normal Consolidation Line (NCL) and Critical State Line (CSL) are plotted in Fig. 11. The slope values of the NCL and CSL are -0.1452 and -0.1498, respectively.

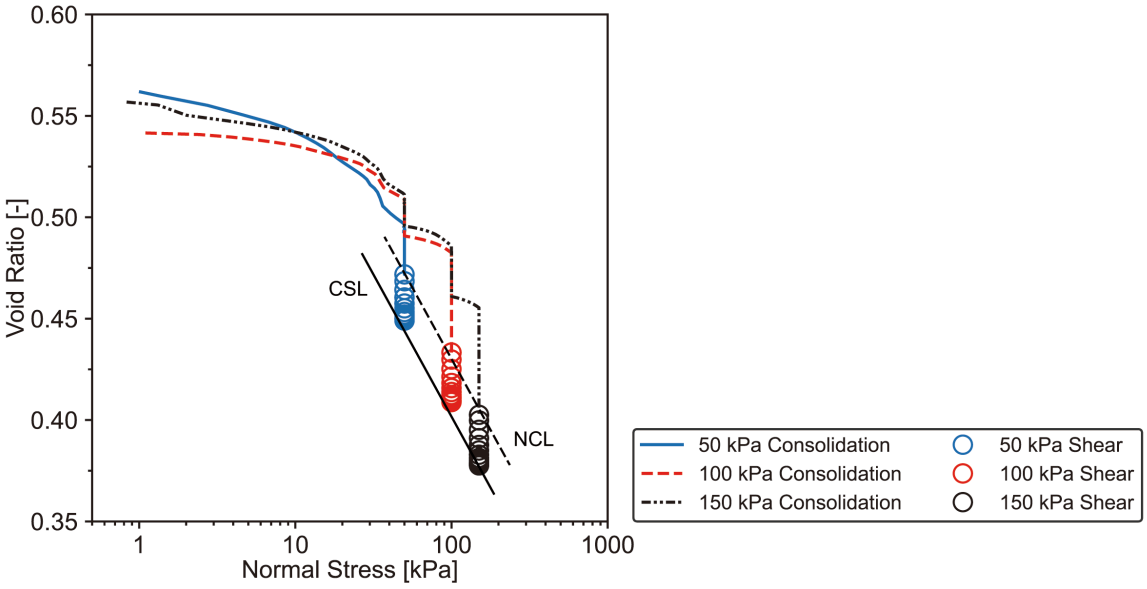

Fig. 11 Void ratio as a function of normal stress during the whole test (consolidation and shear) at 27.5% clay fraction.

5.2.2 Adhesion and friction angle

The residual interface strength is mobilized for a horizontal displacement of about 2 mm. Large displacement is quite often to occur along the soil-pile interface in the pile engineering practice, which corresponds to constant volume (residual) condition of the laboratory interface direct shear test. The residual shear strength is compared in Fig. 12a. For normal stress of 50 kPa, the shear resistance exhibits a quite stable behavior, and ranges between 18.90 kPa and 23.92 kPa with increasing clay fraction. While for higher normal stress of 100

kPa and 150 kPa, the shear strength presents an overall decrease trend with clay fraction increases (Fig. 12a). The residual shear strength of 100 kPa normal stress decreases from 54.50 kPa (0% clay) to 38.05 kPa (55% clay), and the one of 150 kPa normal stress varies from 73.21 kPa (0% clay) to 56.09 kPa (55% clay).

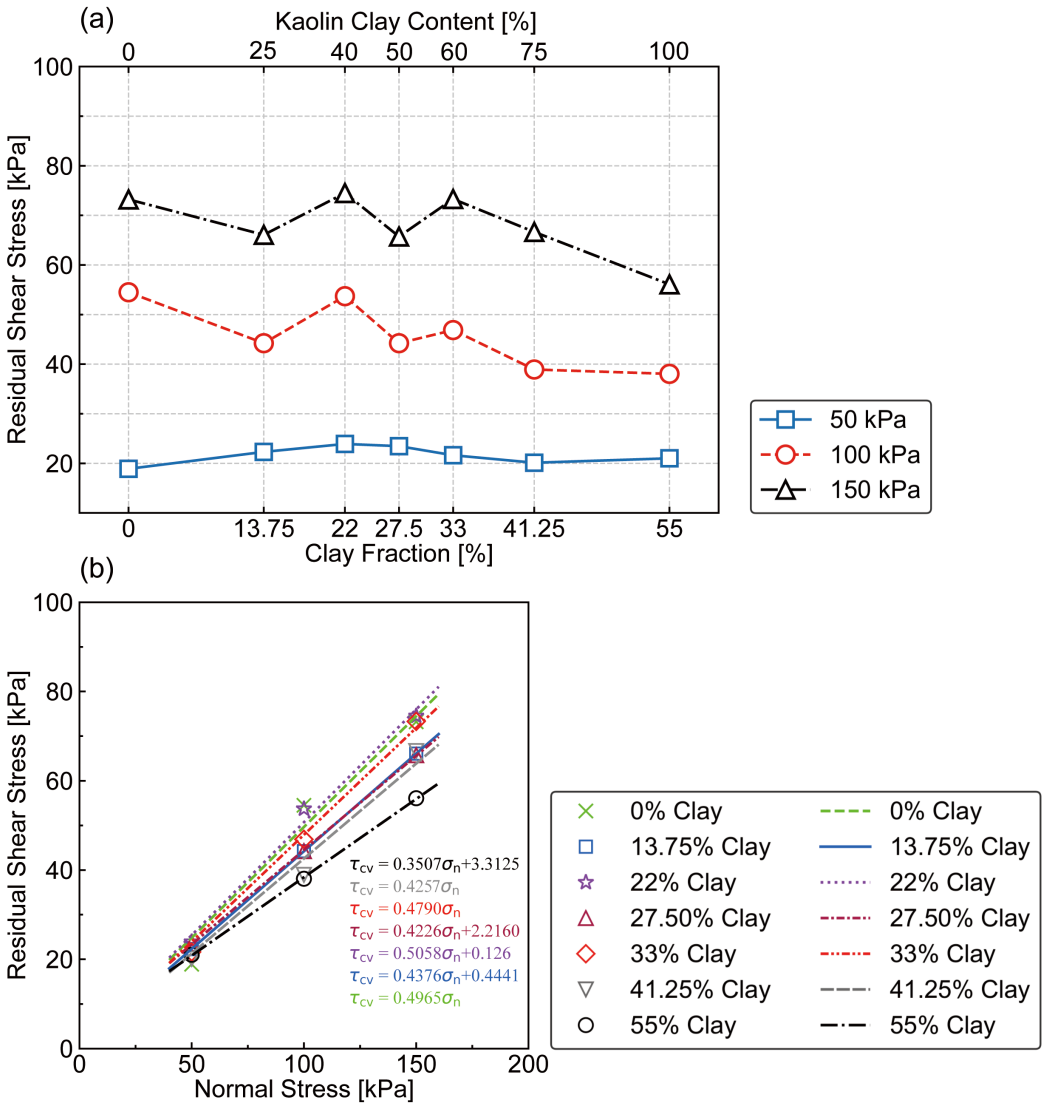

Fig. 12 (a) Residual shear stress as a function of clay fraction and (b) Mohr-Coulomb envelopes in constant volume state.

According to Di Donna (2014) and Li et al. (2019), the adhesion between soil and solid surface is induced by the contact of soil particle-solid surface asperity. Like the cohesion of soil, the adhesion of interface is obtained from the residual Mohr-Coulomb envelope (Fig. 12b).

449 As shown in Fig. 13a, all the residual adhesions are smaller than 5 kPa (some are zero, i.e.,
450 33% and 41.25% clay fraction group), corresponding to the results of saturated NC clayey
451 soils (Di Donna et al. 2016; Potyondy 1961; Vallejo and Mawby 2000; Yavari et al. 2016).
452 Moreover, the adhesion results confirm that the degree of saturation is high enough to
453 consider that the reconstituted samples are fully saturated. For sand under saturated
454 conditions, the cohesion or adhesion is zero (Lu and Likos 2013; Nova 2010). For
455 overconsolidated clay, the adhesion usually has positive values. The cohesion is quite small
456 or even zero for normally consolidated clays (Nova 2010). Concerning the interface between
457 sand-clay mixture and concrete, adhesion is mainly supplied by the contact of clay particles
458 and clay particles-concrete surface in the interface zone. Overall, we can conclude that adding
459 clay to sand may allow the adhesion of the soil-concrete interface to increase a bit (though
460 null values at 33% and 41.25%) as exhibited in Fig. 13a. This is consistent with the test results
461 of sand-clay mixture with different clay fractions, indicating that cohesion increases with
462 increasing clay fraction (Akayuli et al. 2013; Al-Shayea 2001; Balaban et al. 2019). At the
463 55% clay fraction in Fig. 13a, the residual adhesion is 3.3 kPa, only 0.9 kPa lower than the
464 one of the clay (4.2 kPa). With clay fraction increases, a linear relationship is found on the
465 three cohesion values of sand-clay mixtures that are acquired from direct shear tests on soil-
466 soil (Fig. 13a). The 55% clay-concrete interface has quite close residual adhesion (3.3 kPa)
467 with the values from Yavari et al. (2016) (1.8 kPa, kaolin clay-concrete direct shear test) and
468 Di Donna et al. (2016) (7 kPa, illite clay-concrete direct shear test). The red clay-porous stone
469 interface (Li et al. 2019) gives a higher adhesion that is 9.6 kPa in average, due to the different
470 soil type and structural plate.
471 The residual interface friction angles (δ_{cv}) are shown in Fig. 13b, indicating an overall
472 decreasing trend as clay fraction increases, despite two fluctuations at middle clay fractions.
473 The δ_{cv} here has a similar fluctuation with the direct shear results of sand-clay mixture-

structure materials (wood and steel) interface from Aksoy et al. (2016). The reason is that sand can provide higher intergranular friction than clay. In general, the interface friction angle (δ_{cv}) is not the same than soil's internal friction angle (φ_{cv}). In Fig. 13b, the interface soil-concrete friction angles at different clay fractions are compared to the internal friction angles of soils. At 0% clay, the δ_{cv} is 26.4°, 7.3° lower than the φ_{cv} of sand (33.7°). At all clay fractions from 13.75% to 41.25%, the residual interface δ_{cv} values range as 23.6°, 26.8°, 22.9°, 25.6°, 23.1°. At clay fractions of 27.5% and 41.25%, the δ_{cv} is 5.7° and 3.2° lower than the φ_{cv} (28.6° for 27.5%, 26.2° for 41.25%). Whereas at clay fraction of 55%, the gap between δ_{cv} (19.3°) and φ_{cv} (22.5°) is 3.2° (see Fig. 13b).

Even though there is a lack of data on φ_{cv} at three intermediate clay fractions (i.e., 13.75%, 22% and 33%), it is possible to conclude that the δ_{cv} are lower than the φ_{cv}, see also Rouaiguia (2010), Di Donna et al. (2016), Yavari et al. (2016) and Vasilescu (2019). As clay fraction increases, the residual interface friction angles decrease (Fig. 13b), which agrees with previous results of sand-clay mixture in direct shear tests (Balaban et al. 2019; Dafalla 2013; Kim et al. 2018; Phan et al. 2016). The soil internal friction angle is expected to decrease with the increase of clay fraction in the intermediate clay fractions (however we do not have enough experimental results from our campaign, Fig. 13b). To sum up, the friction angle of the soil-concrete interface is smaller than the internal friction angle of the soil (i.e., $\delta_{cv} < \varphi_{cv}$) and it decreases linearly when the clay fraction increases. A subsequent decreasing trend of the δ_{cv} is expected, basing on the overall trend of the δ_{cv} for clay fraction from 0 to 55%, even if there is not any interface direct shear test with the clay fraction higher than 55%. The residual interface friction angle should be close to the 19.33° when clay fraction >55% because the sand-clay mixture is totally clay-controlled.

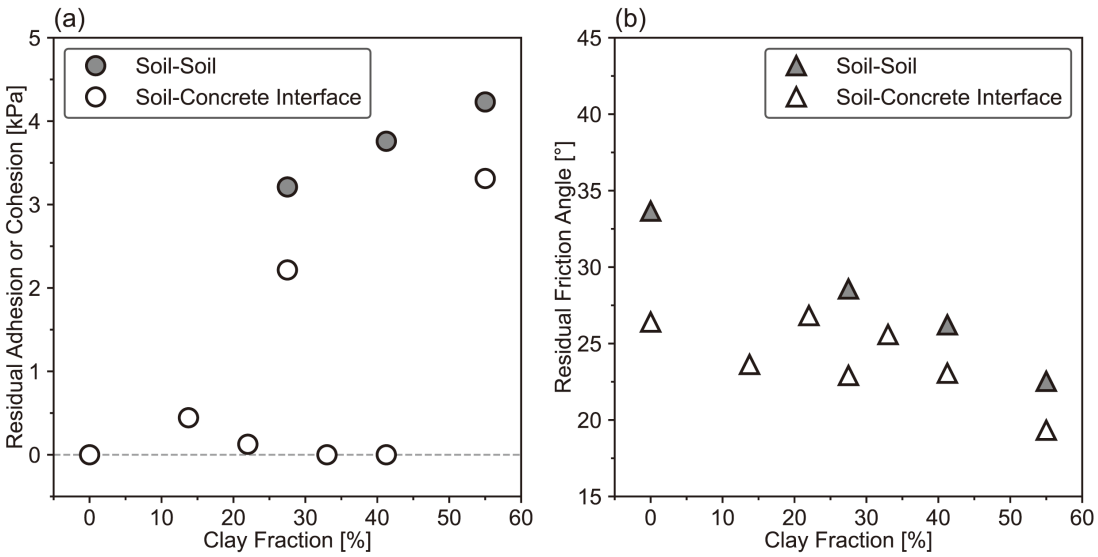

Fig. 13 Comparison between soil-soil and sand-clay mixture-concrete interface direct shear results: (a) adhesion/cohesion and (b) friction angles as a function of clay fraction.

6. Discussion

6.1 Transitional clay content

The clay content (FC) at the condition when the intergranular void ratio (e_g) of the mixture becomes equal to the maximum void ratio ($e_{max\text{-}s}$) of the host granular sand, i.e., $e_g = e_{max\text{-}s}$ can be defined as transition or threshold clay content (Monkul and Ozden 2005; Monkul and Ozden 2007; Yin et al. 2021a; Zuo and Baudet 2015), i.e., FC_t. When $FC > FC_t$, sand grains are expected to be fully separated by clay particles. The maximum void ratio ($e_{max\text{-}s}$) of Fontainebleau sand is 0.866 (Vasilescu et al. 2019; Yin et al. 2019). The intergranular void ratio (e_g) of the sand-clay mixture is calculated according to the method proposed by Monkul and Ozden (2007) and Cabalar and Hasan (2013). As presented in Fig. 14, the FC_t varies with different vertical consolidation stresses (20.93%, 23.73%, and 24.32% at 50 kPa, 100 kPa, and 150 kPa), which is consistent with literature (Cabalar 2011; Monkul and Ozden 2007). The FC_t for the three normal stresses studied is thus around 22%, and it will be used for the shear behavior analysis afterwards.

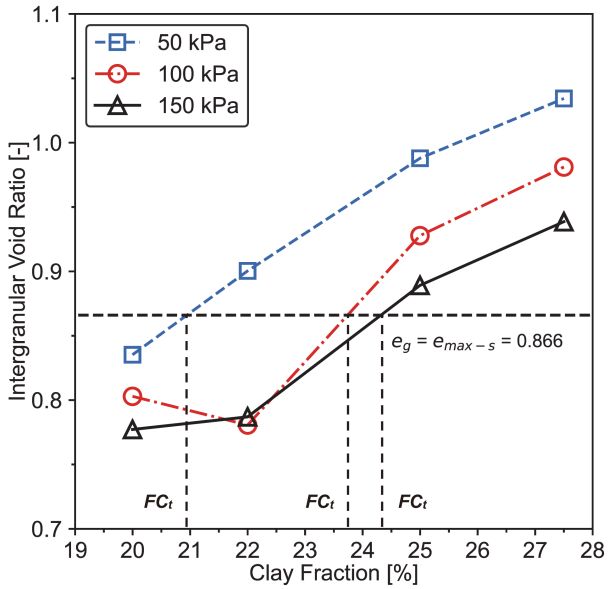

Fig. 14 Intergranular void ratio as a function of clay fraction at different normal stress.

6.2 Comprehensive Analysis

To understand the role of clay on the behavior of soil-concrete interface, the results in terms of shear stress, adhesion, interface friction angle, water content after sample preparation, void ratio after consolidation, and intergranular void ratio are summarized in Fig. 15. A qualitative microstructural analysis is proposed for understanding how the soil particles are arranged at different clay fraction, as well as their influence on the response of sand-clay mixture during interface shearing (Fig. 16).

When a soil sample is sheared, the external force is distributed and carried internally by the soil particles at different scale levels. An internal force chain is formed by the contacts along the boundaries of the soil particles, which transfers the normal stress and sustains the shear forces (Thevanayagam 1998). In sand-clay mixtures, the clay affects and changes the interaction, translation and rolling at the contact boundaries of sand grains. The macroscopic shear response can be interpreted by the sand-clay contacts at the microscopic scale, because the microstructure and internal mechanisms of the forces sustaining affect the macroscopic

behavior during interface shearing (Monkul and Ozden 2007; Thevanayagam 1998; Thevanayagam et al. 2002).

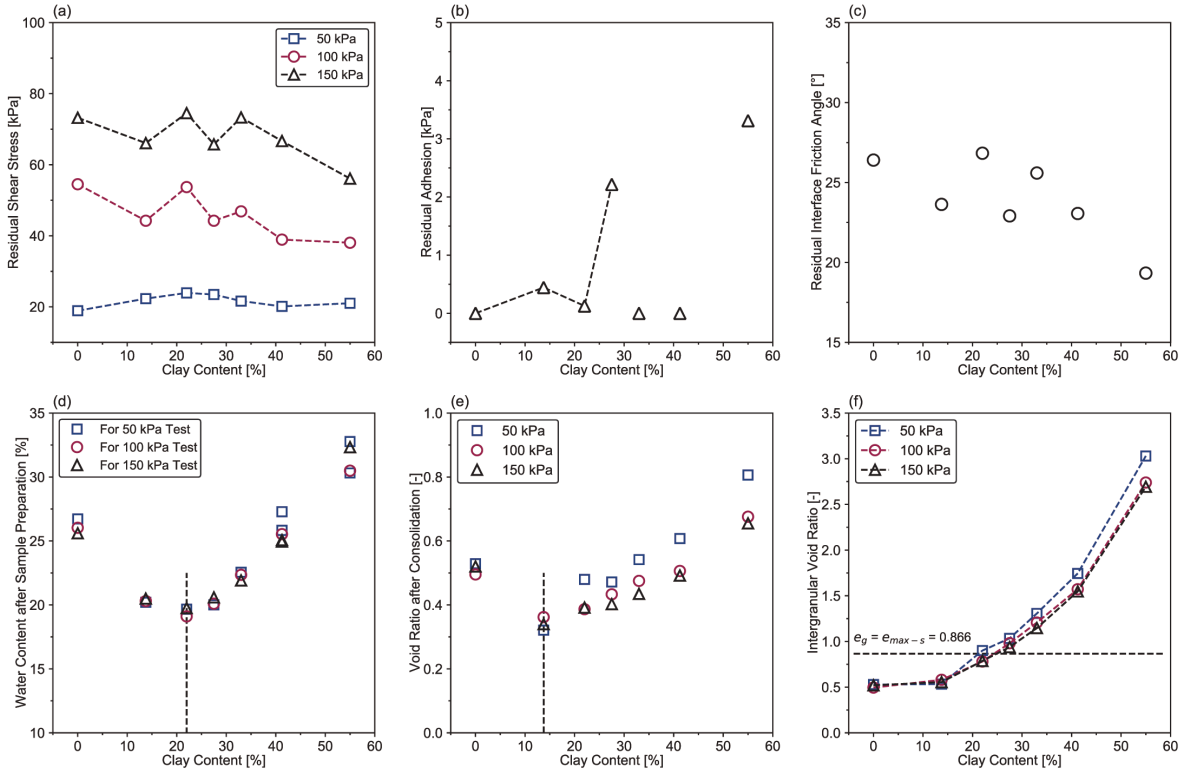

Fig. 15 Comprehensive summary of the interface test results: (a) shear stress, (b) adhesion, (c) interface friction angle, (d) water content after sample preparation, (e) void ratio of specimen after consolidation phase on the interface machine and (f) intergranular void ratio.

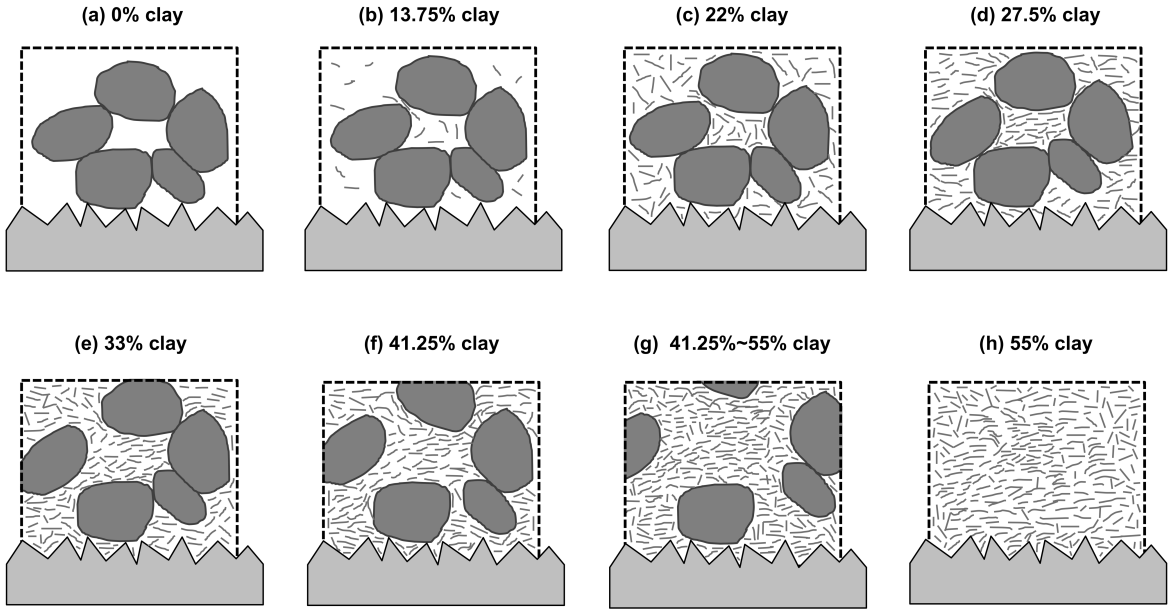

539

540 **Fig. 16 A qualitative microstructural analysis of sand and clay particles in the mixtures on the concrete**
541 **plate at clay fractions of (a) 0%, (b) 13.75%, (c) 22%, (d) 27.5%, (e) 33%, (f) 41.25%, (g) between 41.25%**
542 **and 55%, and (h) 55%.**
543

544

545

When adding clay to sand until 13.75%, the interface behavior begins to change. The void ratio decreases from about 0.5 to the minimum value about 0.33 (Fig. 15e). The residual shear strength of the normal stresses of 100 kPa and 150 kPa test groups decreases about 10 ~ 15 kPa (Fig. 15a). The residual adhesion slightly increases from 0 to 0.4 kPa (Fig. 15b), while the residual interface friction angles decrease with 2.8° (Fig. 15c). From 0% to 13.75%, the intergranular void ratio e_g increases from 0.529 to 0.533 for 50 kPa, 0.495 to 0.581 for 100 kPa, and 0.520 to 0.555 for 150 kPa (Fig. 15f). In order to interpret these results consider Fig. 16a and b: when adding 13.75% clay to the mixture, the clay mainly remains located at the intergranular void of sand (Thevanayagam 1998; Thevanayagam and Mohan 2000), but also a few might exist at the contact points of sandy matrix (Yamamuro and Wood 2004) or form a thin layer coating the sand grains, which is confirmed by the decrease of residual shear stress and friction angle, and adhesion increase (Fig. 15). Hence, the clay between the contact points of sand grains changes the mechanical behavior of the sand-clay mixture along the interface and this result verifies the assumption of sand-fines contact proposed by (Lade et al. 1998). For a clay fraction of 13.75%, a very small quantity of clay particles also stays at the concrete surface roughness profile (Fig. 16b). Besides, though most of the clays are expected to be confined inside the intergranular void space (Thevanayagam 1998), some of the clays still play a secondary role in the transfer of contact forces during shearing; this is verified by the interface δ_{cv} decreasing from 0% to 13.75% clay (Fig. 15c). At this stage, the sand grain still controls the transfer of contact frictional forces.

At clay fraction of 22%, the adhesion slightly decreases (<5 kPa) and there is an increase of void ratio, which means sand and clay are arranging differently from the previous case at 13.75% of clay. The interface friction angle and the residual shear stress increase, indicating that clay actively participates in the interface shearing rather than only the sand. The intergranular void ratio increases and get close to the maximum void ratio of sand (0.866),

571 which means the clay fraction is around the threshold value. At this stage, nearly all
572 intergranular voids between sand grains are filled with clays, and a little bit more clay is still
573 present at the contact zone between sand grains as well. At this clay fraction, more clay
574 particles are stuck in the grooves of the concrete surface roughness than at 13.75% clay
575 fraction (Fig. 16c). Below a clay fraction of 22%, the shear behavior of the sand-clay mixture
576 is mainly sand-controlled.
577 Then after 22% clay, the friction angle, the residual shear stress and the final void ratio
578 increase. More and more clays separate the sand grains, i.e., the sand grains loose contact
579 points from each other (Fig. 16d, e, f). The surface grooves of the concrete plate are more
580 saturated by clay particles than before (R_{max} becomes smaller), which may result in a
581 decreasing normalized roughness of the mixture samples to the plate, the interface thickness
582 becomes thinner. The sand grains are more separated by the clays according to the increase
583 of the intergranular void ratio of the samples (Fig. 15f).
584 From 22% to 41.25%, the response of sand-clay mixture is governed by both sand and clay.
585 When clay fraction goes up, the clay begins to be more dominant than the sand in the sand-
586 clay mixture. The intergranular void space of sand is totally filled up with more and more
587 clay while some sand grains are still in contact with each other (Fig. 16c, d, e, f). According
588 to previous publications (Miftah et al. 2020; Monkul and Ozden 2007), the sand grains should
589 be totally separated after the FC_t. Looking at the interface test results in Fig. 15, however, a
590 part of sand grains is still in contact with each other and can sustain shear force. This is due
591 to the compression effect in both the preconsolidation cell and on the interface device.
592 Assuming that the mixtures' behavior is related to the transitional clay fraction (Cabalar
593 2011; Monkul and Ozden 2005; Monkul and Ozden 2007), the shear behavior of sand-clay
594 mixture is expected to be controlled by clay after the FC_t (about 22%, see Fig. 14), according
595 the direct shear test result from Monkul and Ozden (2007) and Cabalar (2011). Looking at

596 the interface test results of shear strength and friction angle (Fig. 15a, b), however, the
597 mechanical behavior of the interface is controlled by both sand and clay in the clay fraction
598 range from 22% to 41.25%, and not just by clay. After the FC_t, i.e., at the state of $e_g > e_{max\text{-}s}$,
599 a part of the clay acts as the role of secondary load transfer medium (Thevanayagam 1998).
600 Then from 41.25% to 55% clay fraction, the mechanical behavior of the interface is mainly
601 controlled by clay. There is remarkable evidence that the increase of clay fraction from
602 41.25% to 55% affects the adhesion and interfacial friction angle (Fig. 15b, c). Subsequently,
603 at clay fraction of 55%, just the kaolin clay is in contact with the concrete surface, and
604 therefore the interface behavior is dominated by clay. The particles larger than clay particles
605 in the 55% clay group play the same role as sand in this mixture during shearing, clay
606 particles separate all the larger particles and dominate the shear behavior. Moreover, in Fig.
607 15d, the water content after sample preparation (preconsolidation) decreases to a minimum
608 point at 22% clay fraction (19.67% for 50 kPa, 19.11% for 100 kPa, and 19.74% for 150
609 kPa). Then it increases with clay fraction increasing due to the clay particles can hold more
610 water than sand grains. The overall trend of adhesion is that it increases with the clay fraction,
611 while a decreasing trend on the interface friction angles (Fig. 15b, c). The main information
612 can be summarized as follows:
613 (1) the contact between sand grains in the sand-clay mixture changes with increasing clay
614 fraction, especially in the interface zone. Contact between sand-sand grains offers higher
615 shear strength and friction than the one of clay-sand or clay-clay.
616 (2) the number of particles in contact with the concrete plate surface changes with increasing
617 clay fraction, which affects the normalized roughness and consequently the kind of particles
618 (sand or clay) which participate more to the shearing.
619 The shearing of sand involves more rotation of the rotund sand grains, the particle orientation
620 is expected to have negligible effects and finally a higher shear resistance is exhibited

(Rouaiguia 2010). While shearing in clay involves more sliding along clay particles orientation, the smoother shear surface that is formed by strongly oriented clay particles usually exhibits a low shear strength with respect to the case of sand grains (Rouaiguia 2010). Moreover, in the interface shearing with sand-clay mixture, clay particles have lower particle friction than sand grains. With the increase of clay fraction, the shear surface in the interface zone gets smoother since more contact area is taken up by clay particles. The interlocking between sand grains in the rearrangement and rotation process is weakened with the intergranular void ratio increases. The sustaining of force chain transfer changes from sand grains subsequently to both sand and clay, and finally to clay. However, at the normal stress of 50 kPa, the residual shear strength stays nearly constant for all the clay fractions tested.

In conclusion, with the increasing clay fraction from 0% to 55%, the interface shear strength decreases due to the arrangement of clay particles. The size and shape of particles in contact with the concrete plate also affect the shear resistance. The status of contact between sand and clay particles at different clay fractions is identified by the intergranular void ratio and interpreted by the sand-clay contact sketch in Fig. 16.

7. Conclusions

This paper investigates the influence of clay fraction on the direct shear behavior of the interface between reconstituted sand-clay mixture soil and concrete. A method of sample preparation is adopted to prepare the sand-clay mixture specimens for the interface direct shear tests. Test results are presented, compared and discussed. The main findings and conclusions of this research are summarized as follows:

(1) When the clay fraction changes, the contact between sand grains and clay particles changes, especially the particles arrangement in the interface zone. Clay fraction affects the interface behavior and mechanisms through the contact of particles in the sand-clay mixture.

(2) Soil particles in contact with the roughness asperities of concrete surface changes with the variation of clay fraction. This affects the normalized roughness of the concrete. Furthermore, it decides whether the sand grains or the clay particles control the shearing at the interface zone more than the other one.

The experimental results provide information on adhesion and friction angles for sand-clay mixture-concrete interface at different clay fractions, which is a first step to cover the lack of experimental data in the field. To improve the understanding of the interface's mechanical response to shear loading, the interface direct shear experiments should be extended to more boundary and thermo-hydro-mechanical loading conditions to better approach the field conditions. For instance, interface direct shear tests under CNS condition and various (constant or cyclic) thermal loads to continue the present research are encouraged, as started by Vasilescu (2019) on sands.

Data Availability Statement

Some or all data that support the findings of this study are available from the corresponding author upon reasonable request.

Acknowledgments

The research reported in this paper is financially supported by the China Scholarship Council (CSC). The authors would like to express their acknowledgment to M. Mathias Marcel for his technical assistance.

Declarations

The authors declare that they have no known competing financial interests or personal relationships that could have appeared to influence the work reported in this paper.

References

Aboulayt, A., Jaafri, R., Samouh, H., El Idrissi, A. C., Roziere, E., Moussa, R., and Loukili, A. (2018). "Stability of a new geopolymer grout: Rheological and mechanical performances of metakaolin-fly ash binary mixtures." *Construction and Building Materials*, 181, 420-436.

Akayuli, C., Ofosu, B., Nyako, S. O., and Opuni, K. O. (2013). "The influence of observed clay content on shear strength and compressibility of residual sandy soils." *Int J Eng Res Appl*, 3(4), 2538-2542.

Aksoy, H., Inal, E., and Gor, M. "Skin friction between soil and pile materials." *Proc., Proceedings of the 12th International Congress on Advances in Civil Engineering, Istanbul, Turkey*.

Al-Shayea, N. A. (2001). "The combined effect of clay and moisture content on the behavior of remolded unsaturated soils." *Engineering geology*, 62(4), 319-342.

ASTM-D2435 (2011). "Standard test methods for one-dimensional consolidation properties of soils using incremental loading."

ASTM-D3080 (2011). "Standard test method for direct shear test of soils under consolidated drained conditions." *D3080/D3080M*.

Balaban, E., Smejda, A., and Onur, M. "An Experimental Study on Shear Strength Behavior of Soils Under Low Confining Pressure." *Proc., Proceedings of the 4th World Congress on Civil, Structural, and Environmental Engineering*, 1-8.

Cabalar, A., and Hasan, R. (2013). "Compressional behaviour of various size/shape sand–clay mixtures with different pore fluids." *Engineering Geology*, 164, 36-49.

Cabalar, A. F. (2011). "The effects of fines on the behaviour of a sand mixture." *Geotechnical and Geological Engineering*, 29(1), 91-100.

Carraro, J. A. H., and Prezzi, M. (2008). "A new slurry-based method of preparation of specimens of sand containing fines." *Geotechnical Testing Journal*, 31(1), 1-11.

Cerato, A. B., and Lutenegger, A. J. (2006). "Specimen size and scale effects of direct shear box tests of sands." *Geotechnical Testing Journal*, 29(6), 507-516.

Dadkhah, R., Ghafoori, M., Ajalloeian, R., and Lashkaripour, G. R. (2010). "The effect of Scale Direct Shear Tests on The Strength parameters of Clayey Sand in Isfahan city, Iran." *Journal of Applied Sciences*, 18.

Dafalla, M. A. (2013). "Effects of clay and moisture content on direct shear tests for clay-sand mixtures." *Advances in Materials Science and Engineering*, 2013.

Di Donna, A. (2014). "Thermo-mechanical Aspects of Energy Piles." Ph.D. Thesis, École Polytechnique Fédérale de Lausanne (EPFL), Lausanne, Switzerland.

Di Donna, A., Ferrari, A., and Laloui, L. (2016). "Experimental investigations of the soil–concrete interface: physical mechanisms, cyclic mobilization, and behaviour at different temperatures." *Canadian Geotechnical Journal*, 53(4), 659-672.

Eurocode-2 (2004). *Eurocode 2: Design of concrete structures: Part 1-1: General rules and rules for buildings*, British Standards Institution.

Gadelmawla, E., Koura, M., Maksoud, T., Elewa, I., and Soliman, H. (2002). "Roughness parameters." *Journal of materials processing Technology*, 123(1), 133-145.

Hattab, M., Hammad, T., and Fleureau, J.-M. (2015). "Internal friction angle variation in a kaolin/montmorillonite clay mix and microstructural identification." *Géotechnique*, 65(1), 1-11.

Hu, L., and Pu, J. (2004). "Testing and modeling of soil-structure interface." *Journal of Geotechnical and Geoenvironmental Engineering*, 130(8), 851-860.
ISO, E. (1997). "4287–Geometrical Product Specifications (GPS)–Surface Texture: Profile Method–Terms, Definitions and Surface Texture Parameters." *International Organization for Standardization: Geneva, Switzerland*.
Kim, D., Nam, B. H., and Youn, H. (2018). "Effect of clay content on the shear strength of clay–sand mixture." *International Journal of Geo-Engineering*, 9(1), 19.
Krage, C. P., Price, A. B., Lukas, W. G., DeJong, J. T., DeGroot, D. J., and Boulanger, R. W. (2020). "Slurry Deposition Method of Low-Plasticity Intermediate Soils for Laboratory Element Testing." *Geotechnical Testing Journal*, 43(5).
Lade, P. V., Liggio, C., and Yamamuro, J. A. (1998). "Effects of non-plastic fines on minimum and maximum void ratios of sand." *Geotechnical testing journal*, 21, 336-347.
Li, C., Kong, G., Liu, H., and Abuel-Naga, H. (2019). "Effect of temperature on behaviour of red clay–structure interface." *Canadian Geotechnical Journal*, 56(1), 126-134.
Li, L., Fall, M., and Fang, K. (2020). "Shear behavior at interface between compacted clay liner–geomembrane under freeze-thaw cycles." *Cold Regions Science and Technology*, 172, 103006.
Lings, M., and Dietz, M. (2005). "The peak strength of sand-steel interfaces and the role of dilation." *Soils and foundations*, 45(6), 1-14.
Lu, N., and Likos, W. J. "Origin of cohesion and its dependence on saturation for granular media." *Proc., Poromechanics V: Proceedings of the Fifth Biot Conference on Poromechanics*, 1669-1675.
Maghsoodi, S. (2020). "Thermo-mechanical behavior of soil-structure interface under monotonic and cyclic loads in the context of energy geostructures." Université de Lorraine.
Maghsoodi, S., Cuisinier, O., and Masrouri, F. "Thermo-mechanical behaviour of clay-structure interface." *Proc., E3S Web of Conferences*, 10002.
Maghsoodi, S., Cuisinier, O., and Masrouri, F. (2020a). "Effect of Temperature on the Cyclic Behavior of Clay–Structure Interface." *Journal of Geotechnical and Geoenvironmental Engineering*, 146(10), 04020103.
Maghsoodi, S., Cuisinier, O., and Masrouri, F. (2020b). "Thermal effects on mechanical behaviour of soil–structure interface." *Canadian geotechnical journal*, 57(1), 32-47.
Martinez, A., and Stutz, H. H. (2019). "Rate effects on the interface shear behaviour of normally and overconsolidated clay." *Géotechnique*, 69(9), 801-815.
Miftah, A., Garoushi, A. H. B., and Bilsel, H. (2020). "Effects of fine content on undrained shear response of sand–clay mixture." *International Journal of Geosynthetics and Ground Engineering*, 6(2), 1-7.
Monkul, M. M., and Ozden, G. "Effect of intergranular void ratio on one-dimensional compression behavior." *Proc., Proceedings of International Conference on Problematic Soils*, International Society of Soil Mechanics and Geotechnical Engineering …, 27.
Monkul, M. M., and Ozden, G. (2007). "Compressional behavior of clayey sand and transition fines content." *Engineering Geology*, 89(3-4), 195-205.
Nova, R. (2010). *Soil mechanics*, Wiley Online Library.
Phan, V. T.-A., Hsiao, D.-H., and Nguyen, P. T.-L. (2016). "Effects of fines contents on engineering properties of sand-fines mixtures." *Procedia engineering*, 142, 213-220.
Polidori, E. (2007). "Relationship between the Atterberg limits and clay content." *Soils and foundations*, 47(5), 887-896.

766 Potyondy, J. G. (1961). "Skin friction between various soils and construction materials." *Geotechnique*, 11(4), 339-353.
768 Pra-Ai, S. (2013). "Behaviour of soil-structure interfaces subjected to a large number of cycles. Application to piles." Ph.D. Thesis, Université de Grenoble, Grenoble, France.
770 Pra-ai, S., and Boulon, M. (2017). "Soil–structure cyclic direct shear tests: a new interpretation of the direct shear experiment and its application to a series of cyclic tests." *Acta Geotechnica*, 12(1), 107-127.
773 Rouaiguia, A. (2010). "Residual shear strength of clay-structure interfaces." *International Journal of Civil & Environmental Engineering*, 10(3), 6-18.
775 San Nicolas, R., Cyr, M., and Escadeillas, G. (2013). "Characteristics and applications of flash metakaolins." *Applied Clay Science*, 83, 253-262.
777 Seed, H. B., Woodward, R. J., and Lundgren, R. (1966). "Fundamental aspects of the Atterberg limits." *Journal of Soil Mechanics & Foundations Div*, 92(Closure).
779 Shahin, M., Khan, M. M. H., and Bari, M. N. (2020). "A Disaster Resilient Road: Effects of Fines on Density and Shear Strength of Sands." *International Journal of Transportation Engineering and Technology*, 6(2), 38.
782 Thevanayagam, S. (1998). "Effect of fines and confining stress on undrained shear strength of silty sands." *Journal of Geotechnical and Geoenvironmental Engineering*, 124(6), 479-491.
785 Thevanayagam, S., and Mohan, S. (2000). "Intergranular state variables and stress–strain behaviour of silty sands." *Geotechnique*, 50(1), 1-23.
787 Thevanayagam, S., Shenthan, T., Mohan, S., and Liang, J. (2002). "Undrained fragility of clean sands, silty sands, and sandy silts." *Journal of geotechnical and geoenvironmental engineering*, 128(10), 849-859.
790 Tovar-Valencia, R. D., Galvis-Castro, A., Salgado, R., and Prezzi, M. (2018). "Effect of surface roughness on the shaft resistance of displacement model piles in sand." *Journal of Geotechnical and Geoenvironmental Engineering*, 144(3), 04017120.
793 Tsubakihara, Y., Kishida, H., and Nishiyama, T. (1993). "Friction between cohesive soils and steel." *Soils and Foundations*, 33(2), 145-156.
795 Uesugi, M., and Kishida, H. (1986a). "Frictional resistance at yield between dry sand and mild steel." *Soils and foundations*, 26(4), 139-149.
797 Uesugi, M., and Kishida, H. (1986b). "Influential factors of friction between steel and dry sands." *Soils and foundations*, 26(2), 33-46.
799 Uesugi, M., Kishida, H., and Tsubakihara, Y. (1989). "Friction between sand and steel under repeated loading." *Soils and foundations*, 29(3), 127-137.
801 Vallejo, L. E., and Mawby, R. (2000). "Porosity influence on the shear strength of granular material–clay mixtures." *Engineering Geology*, 58(2), 125-136.
803 Vasilescu, A.-R. (2019). "Design and execution of energy piles: Validation by in-situ and laboratory experiments." Ph.D. Thesis, École centrale de Nantes, Nantes, France.
805 Vasilescu, A. R., Fauchille, A.-L., Dano, C., Kotronis, P., Manirakiza, R., and Gotteland, P. "Impact of temperature cycles at soil–concrete interface for energy piles." *Proc., Energy Geotechnics: SEG-2018*, Springer, 35-42.
808 Wang, J., and Gutierrez, M. (2010). "Discrete element simulations of direct shear specimen scale effects." *Géotechnique*, 60(5), 395-409.
810 Wang, S., Luna, R., and Stephenson, R. W. (2011). "A slurry consolidation approach to reconstitute low-plasticity silt specimens for laboratory triaxial testing." *Geotechnical Testing Journal*, 34(4), 288-296.
813 Wichtmann, T., Steller, K., and Triantafyllidis, T. (2020). "On the influence of the sample preparation method on strain accumulation in sand under high-cyclic loading." *Soil Dynamics and Earthquake Engineering*, 131, 106028.

816 Wu, P.-K., Matsushima, K., and Tatsuoka, F. (2008). "Effects of specimen size and some
817 other factors on the strength and deformation of granular soil in direct shear tests."
818 *Geotechnical Testing Journal*, 31(1), 473.
819 Yamamuro, J. A., and Wood, F. M. (2004). "Effect of depositional method on the undrained
820 behavior and microstructure of sand with silt." *Soil Dynamics and Earthquake*
821 *Engineering*, 24(9-10), 751-760.
822 Yavari, N., Tang, A. M., Pereira, J.-M., and Hassen, G. (2016). "Effect of temperature on the
823 shear strength of soils and the soil–structure interface." *Canadian Geotechnical*
824 *Journal*, 53(7), 1186-1194.
825 Yazdani, S., Helwany, S., and Olgun, G. (2019). "Influence of temperature on soil–pile
826 interface shear strength." *Geomechanics for Energy and the Environment*, 18, 69-78.
827 Yin, K., Fauchille, A.-L., Di Filippo, E., Kotronis, P., and Sciarra, G. (2021a). "A Review of
828 Sand–Clay Mixture and Soil–Structure Interface Direct Shear Test." *Geotechnics*,
829 1(2), 260-306.
830 Yin, K., Fauchille, A.-L., Di Filippo, E., Othmani, K., Branchu, S., Sciarra, G., and Kotronis,
831 P. (2021b). "The influence of mixing orders on the microstructure of artificially
832 prepared sand-clay mixtures." *Advances in Materials Science and Engineering*, 2021.
833 Yin, K., Fauchille, A.-L., Othmani, K., Sciarra, G., Kotronis, P., Benoit, Y., Bertrand, F., and
834 Branchu, S. "Influence of sample preparation on the multi scale structure of sand-clay
835 mixtures." *Proc., E3S Web of Conferences*, EDP Sciences, 01007.
836 Yin, K., Liu, J., Lin, J., Vasilescu, A.-R., Othmani, K., and Di Filippo, E. (2021c). "Interface
837 Direct Shear Tests on JEZ-1 Mars Regolith Simulant." *Applied Sciences*, 11(15),
838 7052.
839 Yin, K., Liu, J., Vasilescu, A.-R., Di Filippo, E., and Othmani, K. (2021d). "A Procedure to
840 Prepare Sand–Clay Mixture Samples for Soil–Structure Interface Direct Shear Tests."
841 *Applied Sciences*, 11(12), 5337.
842 Yin, K., Vasilescu, R., Fauchille, A.-L., and Kotronis, P. (2020). "Thermal effects on the
843 mechanical behavior of Paris green clay–concrete interface." *E3S Web Conf.*, 205,
844 13006.
845 Zuo, L., and Baudet, B. A. (2015). "Determination of the transitional fines content of sand-
846 non plastic fines mixtures." *Soils and Foundations*, 55(1), 213-219.
847

List of Figures

873

874 Fig. 8 Direct shear test results of saturated kaolin clay-kaolin clay: (a) shear stress as a
875 function of horizontal displacement, (b) Mohr-Coulomb envelope, and (c) volumetric strain
876 as a function of horizontal displacement.

877

878 Fig. 9 Shear stress as a function of horizontal displacement at (a) 0%, (b) 13.75%, (c) 22%,
879 (d) 27.5%, (e) 33%, (f) 41.25% and (g) 55% clay fractions.

880

881 Fig. 10 Vertical strain as a function of horizontal displacement at (a) 0%, (b) 13.75%, (c)
882 22%, (d) 27.5%, (e) 33%, (f) 41.25% and (g) 55% clay fractions.

883

884 Fig. 11 Void ratio as a function of normal stress during the whole test (consolidation and
885 shear) at 27.5% clay fraction.

886

887 Fig. 12 (a) Residual shear stress as a function of clay fraction and (b) Mohr-Coulomb
888 envelopes in constant volume state.

889

890 Fig. 13 Comparison between soil-soil and sand-clay mixture-concrete interface direct shear
891 results: (a) adhesion/cohesion and (b) friction angles as a function of clay fraction.

892

893 Fig. 14 Intergranular void ratio as a function of clay content at different normal stress.

894

895 Fig. 15 Comprehensive summary of the interface test results: (a) shear stress, (b) adhesion,
896 (c) interface friction angle, (d) water content after sample preparation, (e) void ratio of
897 specimen after consolidation phase on the interface machine and (f) intergranular void ratio.

898

899 Fig. 16 A qualitative microstructural analysis of sand and clay particles in the mixtures on
900 the concrete plate at clay fractions of (a) 0%, (b) 13.75%, (c) 22%, (d) 27.5%, (e) 33%, (f)
901 41.25%, (g) between 41.25% and 55%, and (h) 55%.

902

903

904

905 **List of Tables**

906

907 Table 1 Characteristics of the sensors.

908

909 Table 2 Mix design of the concrete.

910

911 Table 3 Roughness parameters.

912

913 Table 4 Atterberg limits of the sand-clay mixtures.

914

915 Table 5 Sample properties of Fontainebleau sand and kaolin clay for the conventional direct
916 shear tests on soil-soil.

917

918 Table 6 Sample properties after preconsolidation for the soil-concrete interface direct shear
919 tests.

920

921